

Original Research

Transgenic expression of Sag/Rbx2 E3 causes early stage tumor promotion, late stage cytogenesis and acinar loss in the Kras–PDAC model

Qiang Zhang^a; Dongping Wei^a; Mingjia Tan^a; Haomin Li^b; Meredith A. Morgan^a; Yi Sun^{a,c,*}

^aDivision of Radiation and Cancer Biology, Department of Radiation Oncology, University of Michigan, 4424B MS-1, 1301 Catherine Street, Ann Arbor, MI 48109, USA; ^bChildren's Hospital, Zhejiang University School of Medicine, Hangzhou, Zhejiang, China ^cCancer Institute of the Second Affiliated Hospital and Institute of Translational Medicine, Zhejiang University, Hangzhou, China

Abstract

SAG (Sensitive to Apoptosis Gene), also known as RBX2 or ROC2, is a RING component of CRL (Cullin-RING ligase), required for its activity. Our previous studies showed that Sag/Rbx2 co-operated with Kras or Pten loss to promote tumorigenesis in the lung and prostate, respectively, but antagonized Kras to inhibit skin tumorigenesis, suggesting a tissue/context dependent function of Sag. The role of SAG in KRAS-induced pancreatic tumorigenesis is unknown. In this study, we mined a cancer database and found that SAG is overexpressed in pancreatic cancer tissues and correlates with decreased patient survival. Whether Sag overexpression plays a causal role in pancreatic tumorigenesis is unknown. Here, we reported the generation of Sag transgenic mouse model alone (CS), or in combination with Kras^{G12D}, driven by p48-Cre (KCS mice) for pancreatic specific Sag expression. Sag transgenic expression alone has no phenotypical abnormality, but in combination with Kras^{G12D} promotes ADM (acinar-to-ductal metaplasia) conversion *in vitro* and mPanIN1 formation *in vivo* at the early stage, and impairs pancreatic functions at the late stage, as evidenced by poor glucose tolerance and significantly reduced α -Amylase activity, and induction of cytogenesis and acinar cell loss, eventually leading to atrophic pancreata and shortened mouse life-span. Mechanistically, Sag transgenic expression altered several key signaling pathways, particularly inactivation of mTORC1 signaling due to Deptor accumulation, and activation of the antioxidant Nrf2–Nqo1 axis. Thus, Sag plays a stage dependent promotion (early) and fate-changing (late) role during Kras-pancreatic tumorigenesis, likely via regulating its key substrates, which control growth-related signal transduction pathways.

Neoplasia (2020) 22 242–252

Keywords: ADM and mPanINs, Pancreatic tumorigenesis, Kras, SAG, Ubiquitin ligase

Introduction

Pancreatic ductal adenocarcinoma (PDAC) is the third leading cause of cancer death in the USA and one of the deadliest human malignancies with only 5 year survival rate of 9% [1]. Mechanistically, mutational activation of the KRAS oncogene occurs in 95% of cases, along with activation of the EGFR–MAPK and PI3K–AKT–mTORC signaling pathways [2,3]. However, Kras^{G12D} alone does not induce full-blown pancreatic cancer [4]. Therefore, identification of additional genetic alterations that

interact with oncogenic Kras to accelerate the progression of mPanINs to invasive and metastatic PDAC is beneficial for establishing molecular targets for PDAC prevention and therapy.

SAG (Sensitive to Apoptosis Gene), also known as RBX2/ROC2, is the second member of RING family of SCF E3 ubiquitin ligases [5,6]. Although a large number of F-box proteins were found in the human genome [7] that selectively target various protein substrates, there are only two family members of RING proteins in human or mouse, RBX1/ROC1 and RBX2/ROC2/SAG that are required for the ligase activity by transferring ubiquitin from E2 to the substrate [5]. Our previous study using genetic

* Corresponding author at: Division of Radiation and Cancer Biology, Department of Radiation Oncology, University of Michigan, 4424B MS-1, 1301 Catherine Street, Ann Arbor, MI 48109, USA.
e-mail addresses: sunyi@umich.edu, yisun@zju.edu.cn (Y. Sun).

© 2020 The Authors. Published by Elsevier Inc. on behalf of Neoplasia Press, Inc. This is an open access article under the CC BY-NC-ND license (<http://creativecommons.org/licenses/by-nc-nd/4.0/>).
<https://doi.org/10.1016/j.neo.2020.03.002>

modified mouse models revealed that *Rbx1* and *Sag* are not functionally redundant, since total KO of either gene causes embryonic lethality [8,9]. Our recent biochemical-based study showed that RBX1 exclusively binds to ubiquitin E2s CDC34 and UBCH5C to promote substrate polyubiquitylation via the K48 linkage, whereas SAG mainly binds to E2s UBCH10 and UBE2S to promote substrate polyubiquitylation via the K11 linkage [10].

A potential role of SAG in human cancers was first implicated based on its overexpression in various carcinomas of lung, colon, stomach, cervix and liver, and an inverse correlation between SAG overexpression in lung cancer and patient survival [11–15]. To determine whether Sag plays a causal role in tumorigenesis, we have established several lines of mouse models. *Sag* transgenic expression caused early-stage suppression of tumor formation, but later-stage enhancement of tumor growth in skin tumorigenesis induced by DMBA-TPA [16]. In the UVB radiation model, *Sag* transgenic expression promoted skin hyperplasia, but had no significant effect on tumorigenesis [17]. More interestingly, Sag played a tissue- and context-dependent pro-oncogenic or pro-tumor suppressive role in tumorigenesis. Specifically, while *Sag* deletion in the lung and prostate significantly reduced tumorigenesis, triggered by *Kras*^{G12D} or *Pten* loss, respectively [15,18], it accelerated skin tumorigenesis induced by *Kras*^{G12D} [19]. Whether Sag plays a role in pancreas tumorigenesis, and, if so, the underlying mechanisms, is unknown.

In this study, we found that SAG is overexpressed in human pancreatic cancer, which is associated with poor patient survival. To pursue whether SAG overexpression plays a causal role in PDAC, we generated the CS (p48-Cre;Sag-Tg) or KCS (*Kras*^{G12D};p48-Cre;Sag-Tg) mouse models in which Sag transgenic expression alone, or in combination with *Kras* activation in the pancreas, driven by p48-Cre recombinase. We found that while Sag transgenic expression alone has no phenotype, it promotes ADM conversion and mPanIN formation at the early stage, but impairs pancreatic function by inducing cystogenesis and acinar cell loss at the late stage, leading to much shortened life-span. Mechanistically, Sag transgenic expression altered multiple signaling pathways, including inactivation of mTORC1 signaling and activation of the Nrf2-Nqo1 signaling axis. Thus, the role of Sag in pancreatic tumorigenesis induced by *Kras* is stage dependent and likely controlled by its key substrates, which affect several signaling pathways.

Materials and methods

Generation of *Sag* transgenic mice

Transgenic mouse with pancreas-specific overexpression of Sag were generated by using 5.2 kb of the mouse *p48* promoter to drive expression of Sag under control of *LoxP-EGFP-STOP-LoxP* (*p48-LGSL-FLAG-Sag*) sequence (Fig. 2A). Note that the SV40 poly A is used as the transcriptional stop signal for EGFP, while BGH poly A is the stop signal for FLAG-Sag. The Sag transgenic mice were then crossed with *p48*^{Cre/+}; or *p48*^{Cre/+}; *Kras*^{G12D/+} mice (referred to hereinafter as KC mice) to create mice with Sag overexpression and *Kras* activation in pancreas, driven by p48-Cre recombinase (designated as KCS mice). Genotyping was carried out by tail clipping from mice 2 weeks after birth. The primers used for genotyping were: *Kras*^{G12D}-F: 5'-AGGTAGCCACCATGGCTTGAGTAAGTCTGCA-3'; *Kras*^{G12D}-R: 5'-CCTTTACAAGCGCACGCA GACTGTAGA-3'; Cre-F: 5'-GAACCTGATGGACATGTTTCAGG-3'; Cre-R: 5'-AGTGCCTTCAACGCTAGAGCCTGT-3'; p48-Sag EGFP-F: 5'-AATCTCGAGGCCACCATGGTGAGCAAGGGC GAGGA-3'; p48-Sag EGFP-R: 5'-TACTTGTACAGCTCGTC CATGCCGAGAGTGATC-3'. All procedures were approved by the University of Michigan Committee on Use and Care of Animals. Animal care was provided in accordance with the principles and procedures out-

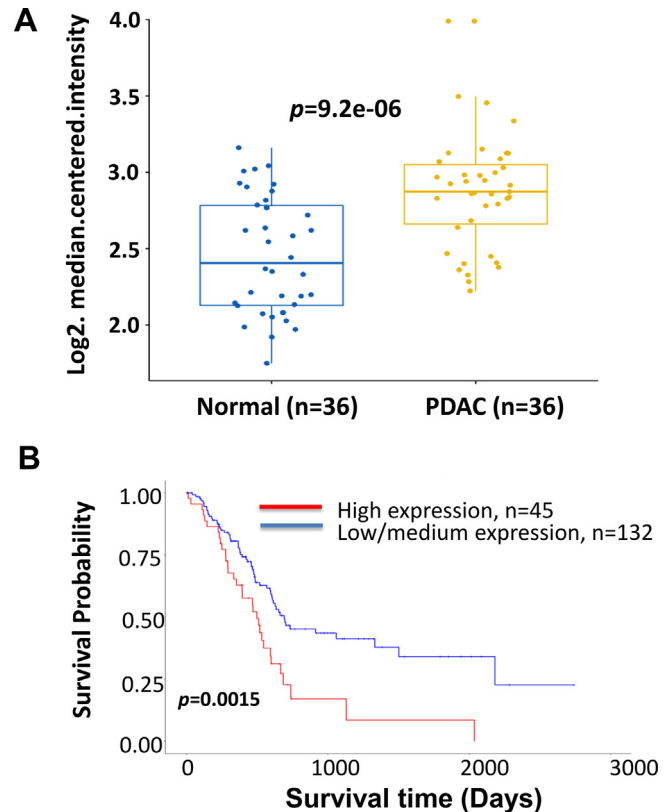


Fig. 1. SAG is overexpressed in human PDAC and correlates with poor patient survival. (A) The scatter plot displays the differential expression levels of *SAG* transcripts in paired PDAC and non-cancer pancreas tissues for the GSE15471 dataset. (B) Kaplan–Meier curve to show the association between the levels of SAG expression and overall survival of patients with PDAC.

lined in the National Research Council Guide for the Care and Use of Laboratory Animals.

Cell line and characterization of *p48-LGSL-FLAG-Sag* in vitro

Mouse pancreatic acinar cell line 266-6 was obtained from the American Type Culture Collection. Cells were cultured in Dulbecco's modified Eagle medium supplemented with 10% FBS, 2 mM glutamine, and antibiotics. Cells were transfected with p48-LGSL-FLAG-Sag by Lipofectamine 2000 (Invitrogen) according to the manufacturer's protocols. Transfected 266-6 cells were further infected with Ad-Cre (adenovirus encoding Cre recombinase) to delete the EGFP-STOP segment DNA flanked by LoxP and get FLAG-Sag expression.

Oral glucose tolerance test and amylase activity assay

For glucose tolerance tests, 6-month KC and KCS mice were fasted overnight (14 h) then injected i.p. with glucose (2 g/kg). Tail vein blood glucose was measured using a blood glucose meter (Roche Diagnostic) at 0, 15, 30, 60, and 120 min after injection. For Amylase activity assay, pancreata from 6-month KC and KCS mice were prepared and the amylase activity was determined by using an amylase activity assay kit (Sigma-Aldrich), which results in a colorimetric (405 nm) product. The amylase activity is proportional to the amount of substrate (ethylidene-pNP-G7) cleaved by the amylase.

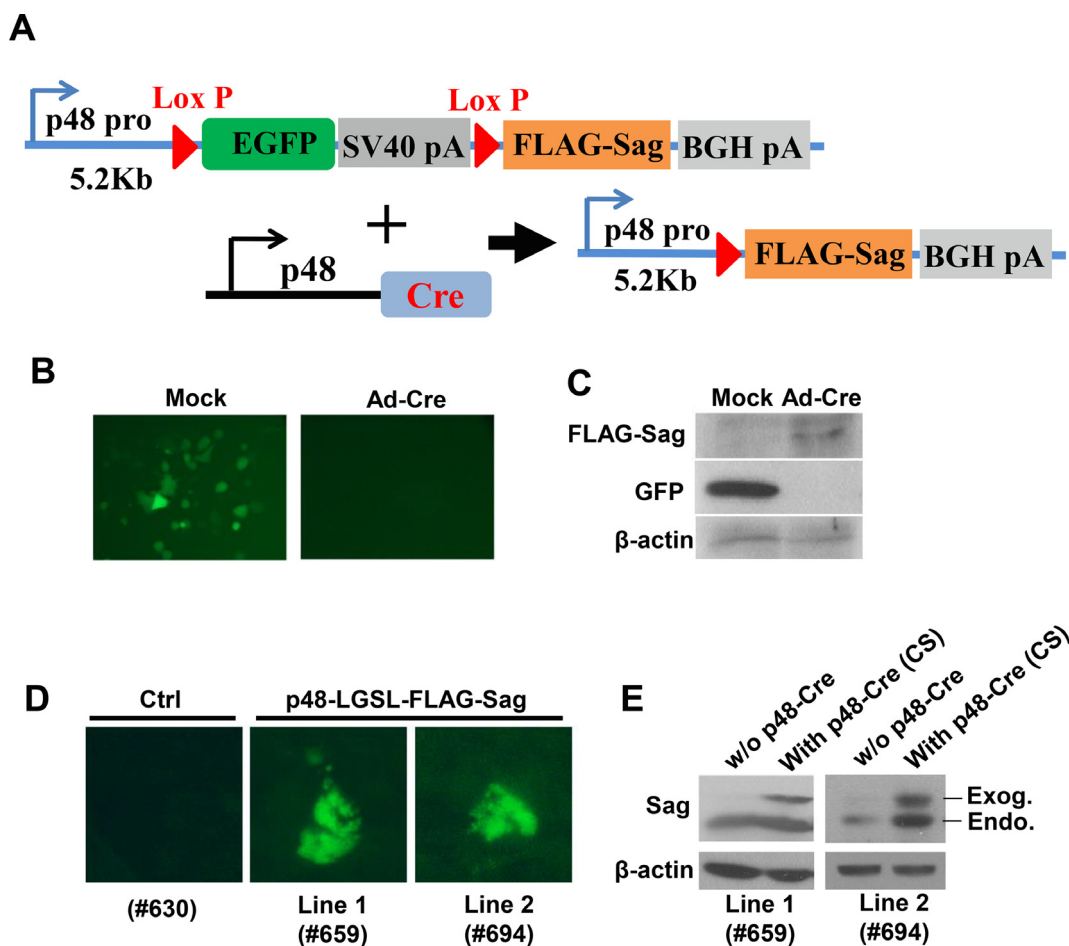


Fig. 2. Characterization of KC-Sag (KCS) transgenic mice. (A) Genetic makeup of the KCS mice. A 5.2 kb mouse p48 promoter-driven FLAG-Sag expression cassette is inserted with flanking LoxP sites which have EGFP-STOP sequence in the middle. Upon crossing to a p48-Cre mouse line to remove EGFP-STOP fragment, FLAG-Sag is strictly expressed in mouse pancreata. (B) p48-(LoxP-EGFP-STOP-LoxP)-FLAG-Sag construct was transfected into mouse pancreatic acinar tumor cells 266-6 and EGFP expression was observed (Mock). Upon Ad-Cre infection for 48 h, EGFP fluorescence was not detected (Ad-Cre), indicating an excision of EGFP-STOP cassette due to LoxP recombination. (C) The cells in panel (B) were collected for immunoblot analysis. FLAG-Sag was detected in Ad-Cre infected 266-6 cells while EGFP protein was only observed in control (Mock) cells. (D) Pancreata from one control mouse (without p48-LGSL-FLAG-Sag transgene) and two independent p48-LGSL-FLAG-Sag founders (Line 1: #659; Line 2: #694) were collected for detecting EGFP expression by fluorescence. (E) Immunoblotting analysis showed that transgenic expression of FLAG-Sag was found in both transgenic lines upon crossing with p48-Cre mice, but not detected in the littermates without p48-Cre allele.

Immunohistochemistry and immunoblotting

Pancreatic tissues were fixed in 10% formalin and embedded in paraffin. Five- μ m-thick sections were cut for H&E and immunohistochemistry staining. Immunohistochemistry was conducted as previously described [20]. Images were acquired with an Olympus BX-51 microscope, Olympus DP71 digital camera, and DP Controller software. Antibodies used for immunohistochemistry include those recognizing Ki67 (BD Bioscience, Cat. 550609, 1:500), CK19 (Abcam, ab87000, 1:500), and Amylase (Sigma-Aldrich, A8273, 1:500), Muc5A (Abcam, ab3649, 1:1000), p-S6K (Novus, NB600-1049, 1:200), p-4EBP1 (Cell Signaling, #2855, 1:200), p-mTOR (Cell Signaling, #2976, 1:100), c-JUN (Cell Signaling, #9165, 1:200), Erbin (Abcam, ab124653, 1:100), Nqo1 (Santa Cruz, sc-32793, 1:100). The immunoblotting analysis was performed as described [21]. Antibodies used include those recognizing EGFP (Abcam, ab13970, 1:1000), SAG (clone: Sag-10) [13,21], β -TrCP (Cell Signaling, #4394, 1:1000), DEPTOR (Cell Signaling, #11816, 1:1000), p-Erk1/2 (Cell Sig-

nal, #9101, 1:1000), Erk1/2 (Cell Signaling, #9102, 1:1000), NRF2 (Cell Signaling, #12721, 1:1000), FLAG (Sigma, A2220, 1:2000), and β -actin (Sigma Aldrich, Clone AC-40, 1:5000).

Acinar cell culture

The 3D culture of pancreatic acinar cells was prepared by digesting pancreata from 2-month-old mice with Collagenase P and then culturing in Matrigel as previously described [20]. Briefly, pancreata from KC, KCS, and control mice were cut into small pieces and digested with 2 mg/ml of Collagenase P (Roche Diagnostics) in HBSS for 15 min at 37 °C. Cells were then washed three times with HBSS with 5% FBS and filtered through 100- μ m nylon meshes. After centrifugation, the cell suspension was mixed 1:1 with Matrigel and plated onto the collagen layer. The acinar cell/Matrigel mix was allowed to solidify for 1 hour at 37 °C before adding medium. The formation of duct-like structures was observed at days 1, 2, and 3.

Histopathologic analysis

Histopathologic analysis was conducted by a pathologist at the University of Michigan (Dr. Ingrid Bergin) on all deidentified hematoxylin and eosin (H&E)-stained slides. Pancreata sections were evaluated for ADM, PanIN1, PanIN2, PanIN3, and PDA lesions based on a previously reported classification system [4]. Pancreata were diagnosed according to the most severe phenotype observed, and data were expressed as the percentage of animals with each phenotype.

Statistical analysis

Survival curves were calculated according to the Kaplan–Meier method, and statistical differences were analyzed by the log-rank and Gehan–Breslow–Wilcoxon tests using GraphPad Prism. A two-sided, unpaired Student's *t* test was used for other statistical analyses. The *p* values of <0.05 were considered statistically significant.

Results

SAG is overexpressed in human PDAC, which correlates with poor patient survival

Previous studies from our laboratory and others have shown that SAG is overexpressed in a panel of human tumor tissues, including lung, colon, stomach, and liver, as compared to paired normal tissues, and SAG overexpression in lung cancer is positively correlated with poor survival of patients [11–15]. To determine potential alterations of SAG expression in human PDAC samples, we performed a datamining analysis in the Gene Expression Omnibus (GEO) database. In a study containing 36 paired human PDAC samples and their non-cancer pancreas tissues (GSE15471), *SAG* expression is significantly higher in the PDAC samples in comparison to the normal pancreas [22] (Fig. 1A). To associate SAG overexpression with patient survival, we performed the survival analyses of PDAC patients in TCGA based on *SAG* expression levels (High vs. Low/medium). According to the log-rank test from Kaplan–Meier survival analysis, high expression of *SAG* is associated with poor overall survival of the PDAC patients (<http://ualcan.path.uab.edu/cgi-bin/TCGA-survival1.pl?genenam=RNF7&cctype=PAAD>) (Fig. 1B). Thus, *SAG* is indeed overexpressed in human PDAC tissues and *SAG* overexpression may serve as a novel prognostic biomarker for PDAC patients.

Construction and characterization of Kras^{G12D};p48-Cre;FLAG-Sag (KCS) mouse model

KRAS mutations occur in almost all PDAC tissues, and mutated KRAS initiates pancreatic tumorigenesis and drives PDAC development [24,25]. To investigate if SAG overexpression seen in PDAC tissues indeed plays a causal role in pancreatic tumorigenesis triggered by KRAS mutation, we generated a Sag transgenic mouse model using 5.2 kb of the mouse pancreas-specific transcription factor 1 (Ptf1a)/p48 promoter to drive expression of FLAG-tagged Sag under control of LoxP-EGFP-STOP-LoxP (p48-LGSL-FLAG-Sag) sequence with the SV40 poly A being used as the transcriptional stop signal for EGFP, whereas the BGH poly A as the stop signal for FLAG-Sag (Fig. 2A). To validate that the p48-LGSL-FLAG-Sag transgene was working properly, we first characterized the transgene by transfecting it into a mouse pancreatic acinar cell line 266-6. Indeed, the cells transfected with p48-LGSL-FLAG-Sag construct exhibited high EGFP expression, whereas EGFP expression was completely abrogated in the same cells infected with Ad-Cre (adenovirus encoding Cre recombinase) which resulted in removal of the EGFP encoding sequence (Fig. 1B). FLAG-Sag expression and EGFP depletion was

further confirmed by immunoblotting in 266-6 cells transfected with p48-LGSL-FLAG-Sag upon Ad-Cre infection (Fig. 2C), suggesting that transgenic construct is working, as expected.

To exclude the possibility of an off-target effect, we selected 2 independent transgenic lines (#659 and #694) for further studies. Compared to a control line (#630, without p48-LGSL-FLAG-Sag transgene), both transgenic lines expressed EGFP protein in the pancreas (Fig. 2D). We then crossed the p48-LGSL-FLAG-Sag mice with the KrasLSL^{G12D/+};p48^{Cre/+} mice (designated as KC) to create pancreas-specific Sag transgenic expression in the KC background (designated as KCS) as well as the p48-Cre; p48-LGSL-FLAG-Sag (designated as CS) mice. We determined FLAG-Sag expression in both lines upon introduction of p48-Cre allele in the pancreas and found that exogenous FLAG-Sag is indeed expressed, and to the levels similar to the endogenous Sag (Fig. 2E). Taken together, these results clearly show that p48-Cre drives FLAG-Sag expression in the pancreatic tissues of compound mice.

Sag transgenic expression cooperates with Kras mutation to trigger pancreatic atrophy and shorten the life-span

Both lines of KCS mice were born with expected Mendelian frequency. While CS mice with Sag transgenic expression without Kras^{G12D} did not show any abnormality up to adulthood, the KCS mice started to show the signs of growth retardation with a hunched-posture after 4-5 months of age. We, therefore, dynamically observed the body weight of CS, KC, and KCS mice in both genders and found that KCS mice started to lose body weight at around 15 weeks with significant weight loss at week of 30, which is sex-independent (Fig. 3A). Indeed, KCS mice have smaller body size, and the pancreata from the KCS mice were much smaller and atrophic (Fig. 3B). The pancreas/body (w/w) ratio was significantly reduced in KCS mice as compared to the KC mice, while the other organs in KCS mice were proportional to mouse weight, except for the spleen which also had a smaller ratio (Fig. 3C and D). Survival of CS, KC and KCS (two independent lines) mice was monitored for up to 600 days. Remarkably, the KCS mice (both lines) had significantly shortened life-span, compared to the KC mice (Fig. 3E). In line with these growth-retarded and pancreas-atrophic phenotypes, most KCS mice became ill and had to be euthanized between 8 and 10 months. The biochemical analyses of KCS mice revealed signs of diabetes with much higher values in the glucose tolerant test (GTT) (Fig. 3F), and reduced α -Amylase levels in the sera (Fig. 3G). Thus, it is likely that KCS mice may die of defective pancreatic functions before fully developing PDAC. Taken together, these results clearly showed that Sag transgenic expression in combination with Kras^{G12D} activation significantly retards pancreatic development, and impairs pancreatic functions, which certainly contributes to the shortened life-span.

Sag transgenic expression promotes early mPanIN formation, followed by pancreatic cystogenesis with the loss of acinar structures

To determine the potential effect of Sag-transgenic expression on Kras-induced pancreatic tumorigenesis, we histologically assessed the pancreata from KCS mice at 2, 4, and 6 months of age. At 2 months of age, increased numbers of mPanIN1a/1b structures were evident in KCS mice, but not in KC mice. At 4 months of age, more mPanIN1a/1b structures were found, along with the appearance of cystic structures in the KCS mice, whereas only some scattered mPanIN1 structures started to show in the KC mice. Remarkably, at the age of 6 months, although the extent of mPanINs and cysts in the pancreata of KCS mice varies, most of KCS mice showed profound cystic structures with limited mPanIN1 structures and an overall loss of normal acinar cells and islets, while the KC mice developed some of mPanIN2-3 structures and maintained normal acinar

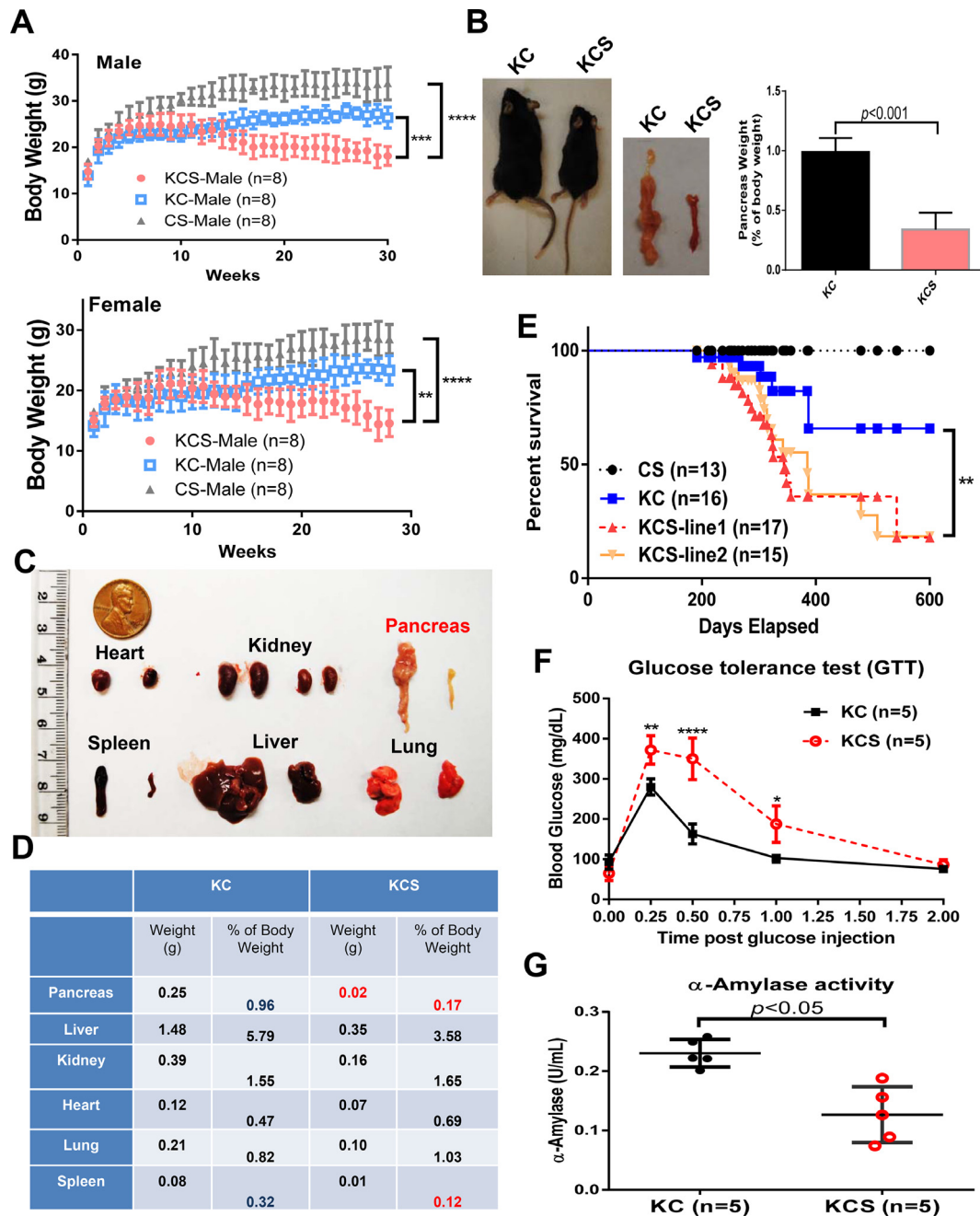


Fig. 3. KC-Sag transgenic mice show shorter life-span with impaired pancreatic functions. (A) Dynamic body weight of male (upper) and female (lower) KCS, KC, and CS mice. KCS mice show reduced body weight from ~15 weeks in both genders. (B) Macroscopic comparison of KCS mouse versus their KC littermate at the age of 6 months (Left); Dramatic pancreatic hypoplasia was observed in KCS mice compared with KC mice (Middle); Loss of pancreatic weight relative to total body weight in KCS mice indicates significant pancreatic atrophy (Right). (C and D) Overall profile of main organs (including heart, kidney, lung, liver, spleen, and pancreas) of KC and KCS mice; the organ weight/body weight ratio was calculated in one KC and one KCS mice at 8 months old, suggesting pancreatic atrophy in KCS mice. (E) Pancreas-specific Sag expression in two independent lines leads to shorter life-span. The survival of CS, KC, KCS-line1, and KCS-line2 mice is expressed using the Kaplan-Meier method, and statistically significant differences from KC mice are shown ($P < 0.01^{**}$) in both lines. (F) Glucose tolerance testing in the 6-month KC and KCS mice suggests impaired glucose tolerance in KCS mice ($n = 5$). (G) Pancreatic amylase activity in the serum of KC and KCS mice. The enzymatic activity of α -Amylase is significantly reduced in the KCS mice ($n = 5$) at 6 months old.

structures (Fig. 4A). Consistent with the H&E staining and serum α -Amylase activity assay, the immunohistochemistry staining revealed that the acinar cell marker α -Amylase was almost completely lost in the pancreata of KCS mice at 6 months, compared to their KC littermates (Fig. 4B,

left). While the expression of cytokeratin 19 (CK19), a biomarker for duct-like lesions in PDAC [23], showed comparable levels (Fig. 4B, middle), the expression of Muc5AC, a marker for invasive progression of PDAC [24], was remarkably reduced in the KCS mice, compared to the

KC littermates (Fig. 4B, right). We further assessed the proliferative marker Ki67 and found significantly decreased levels of Ki67 in KCS pancreata (Fig. 4C), which is in agreement with acinar cell loss and pancreas atrophy. Taken together, these results demonstrate that Sag transgenic

expression promotes the mPanIN formation at the early stage, followed by cystogenesis which severely damages the acinar structures and impairs the proliferation and normal function of the pancreas, leading to an atrophic and diabetic phenotype and shortened mouse life-span.

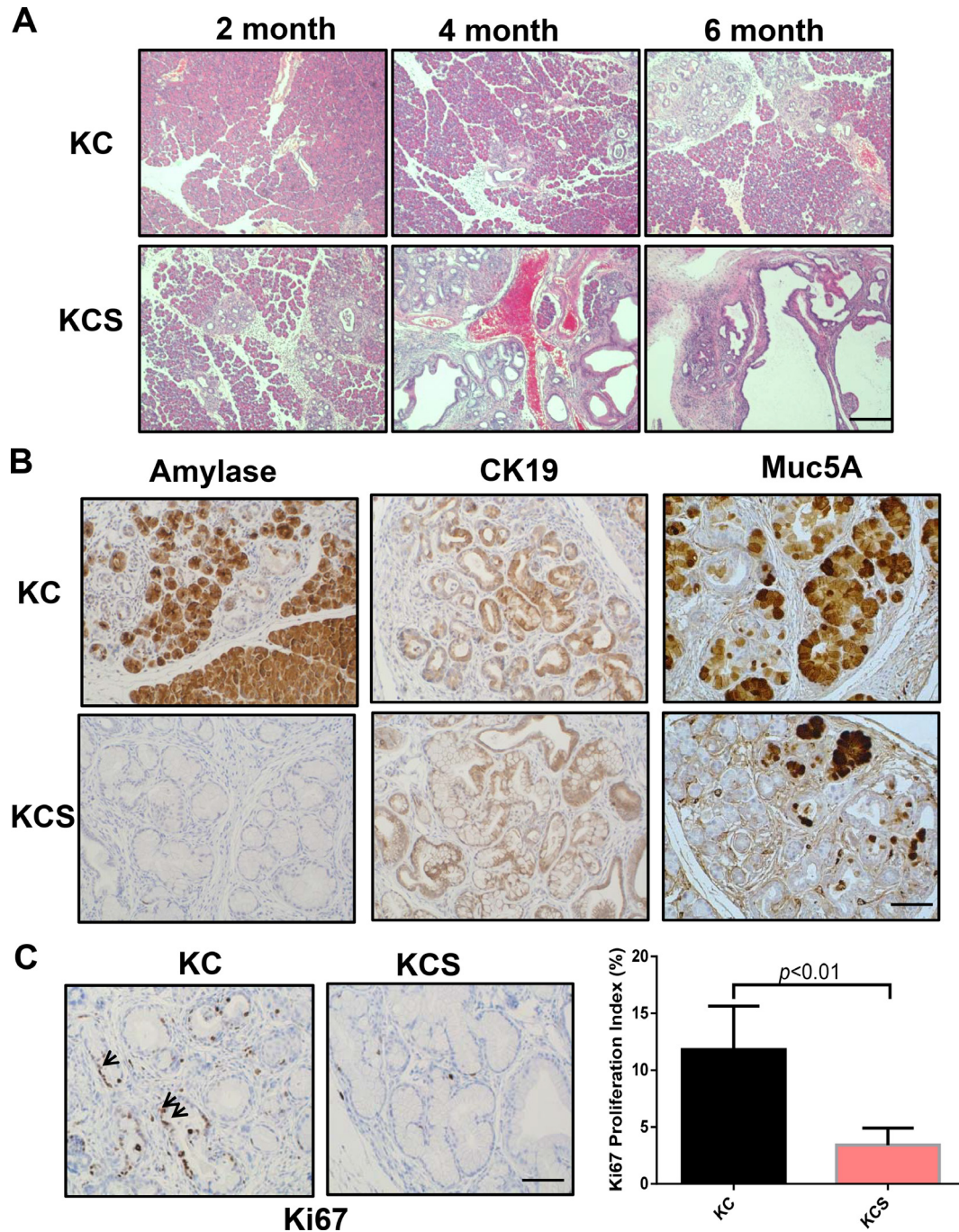


Fig. 4. KC-Sag transgenic mice show accelerated PanIN formation at early stage, and cystic structures in the later stage. (A) H&E staining of pancreata of KC and KCS mice at 2, 4, and 6 months. Scale bar, 100 μ m. Each image is representative of at least three independent animals. (B) Immunohistochemical assessment of Amylase, CK19, and Muc5A in KC and KCS pancreata at 6 months. Scale bar, 100 μ m. (C) Immunohistochemical assessment of Ki67 in KC and KCS pancreata at 6 months. Scale bar, 100 μ m (Left). Quantitation of Ki67-positive cells in each of the indicated genotypes (Right). Five randomly selected, nonoverlapping high-power images (20 \times objective) were taken from each slide of each group. Nuclei positive for Ki67 were counted as actively proliferating cells. Data are the mean percentage of total counted nuclei for each of 5 randomly selected fields \pm SE ($p < 0.01^{**}$).

Sag transgenic expression accelerates acinar-to-ductal metaplasia conversion with enlarged duct-like structures

The early appearance of the mPanIN1 structure could imply a rapid and profound earlier onset of ADM in KCS pancreata. To confirm the ADM acceleration by Sag transgenic expression, we used the 3D cultures of acinar clusters and found the formation of duct-like structures as early as 1 day in KCS mouse acini. A higher percentage was also found in acinar cells from KCS, as compared to those from KC (Fig. 5A and B). Remarkably, the duct-like structures from KCS acini have a much larger size at day 2 and 3, which is consistent with the observed increase in PanIN lesions *in vivo* (Fig. 5A and C). These data suggest that Sag transgenic expression cooperates with mutant Kras to promote ADM conversion at the early stage. The larger size of duct-like structure may be associated with later stage of cystogenesis seen in the pancreata of KCS mice.

Sag transgenic expression dysregulates multiple signaling pathways

SAG/RBX2, is the RING component of the Cullin-RING ligases (CRLs), and specifically for SCF/CRL1 and CRL5 which promote the ubiquitylation and degradation of many key signaling molecules to regulate a number of cellular processes [5]. We previously showed that Sag promotes the ubiquitylation and degradation of c-Jun, I κ B α , p27, and Erbin to regulate skin tumorigenesis [16,17,19,21], and apoptosis [25], HIF-1 α for hypoxia regulation [26], and β -TrCP to regulate its substrates [10]. We next sought to examine the protein levels of some key substrates in the pancreata from two independent KCS and KC mice, respectively. Immunoblotting analysis revealed that Sag transgenic expression significantly reduced the levels of Erbin, an inhibitor of Ras activation of Raf [19], HIF-1 α , and β -TrCP1, moderately reduced the levels of c-Jun, but had no effect on I κ B α and p27 (Fig. 6A, top panels), suggesting a context dependent degradation of known Sag substrates. Decreased levels of

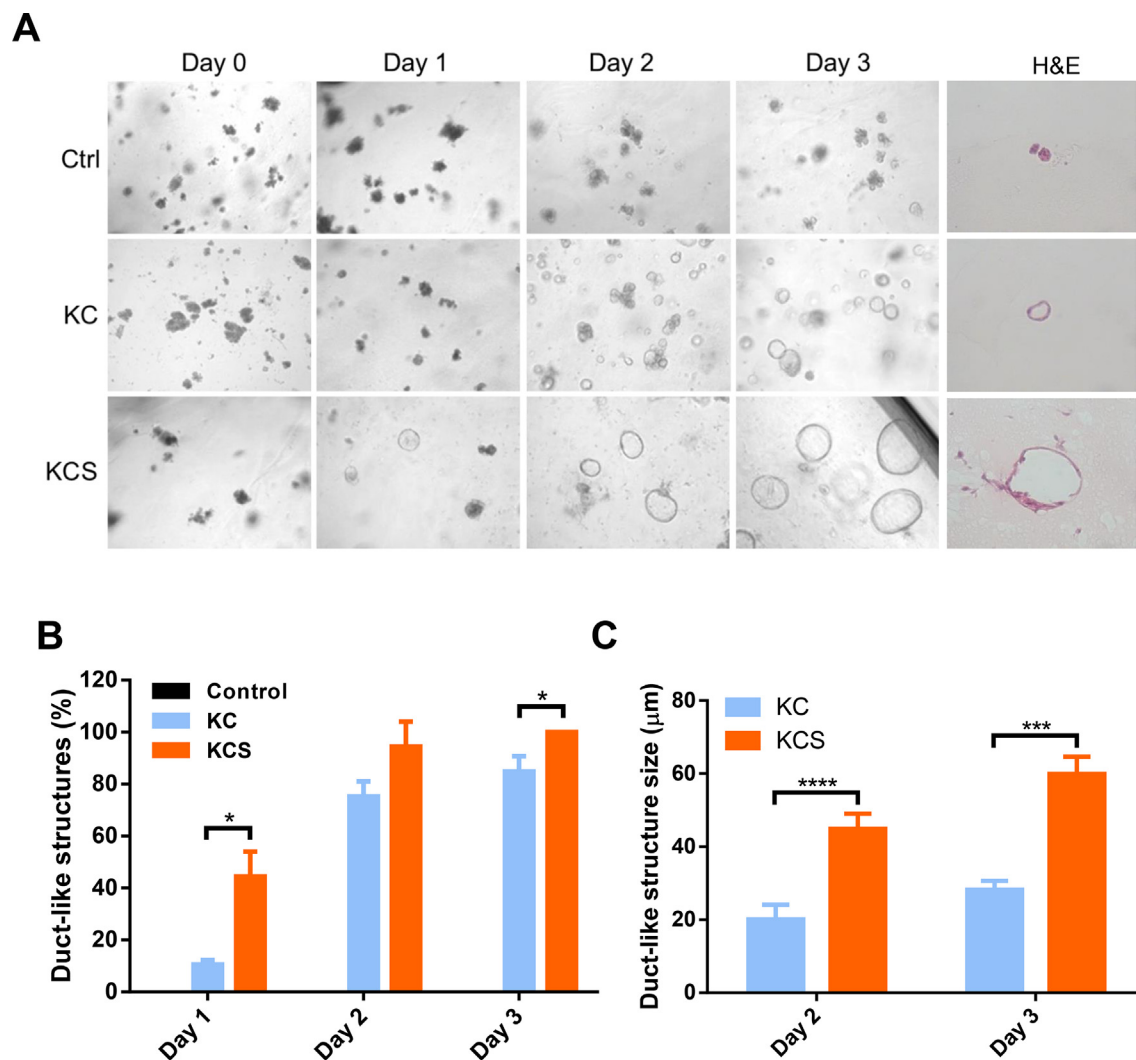


Fig. 5. Sag transgenic expression accelerates ADM conversion and enlarges the size of duct-like structures *in vitro*. (A) Transmitted light images of control, KC, and KCS pancreatic cell clusters in 3D culture from day 0 to 3 are shown. H&E staining of control, KC, and KCS pancreatic cell 3D structures at Day 3. Scale bar, 100 μ m. (B) Quantification of duct-like structures. Statistically significant differences were determined by a two-sided, unpaired Student's *t* test and are indicated ($p < 0.05^*$). (C) Quantification of the size of duct-like structure of KC and KCS mice. Statistically significant differences were determined by a two-sided, unpaired Student's *t* test and are indicated ($p < 0.001^{***}$, $p < 0.0001^{****}$).

Erbin and c-Jun were also confirmed by immunohistochemistry staining (Fig. 6B).

In line with reduction of β -TrCP1, we observed accumulation of Deptor, a well-known substrate of β -TrCP1 [27–29], and a naturally occurring inhibitor of both mTORC1 and mTORC2 [30]. Indeed, consistent with Deptor accumulation, mTORC1 signaling was significantly inactivated in KCS pancreata tissues, as evidenced by decreased levels of p-mTOR, p4EBP1, pS6K (Fig. 6A, middle panels), which was further confirmed by reduced levels of pS6K, p4EBP1 and p-mTOR assessed by immunohistochemistry staining (Fig. 6B). Finally, we found that while it had minor, if any, effect on the Ras-MAPK pathway, Sag transgenic expression caused significant accumulation of Nrf2, an antioxidant transcription factor [31] with a corresponding increase in its downstream target, Nqo1 (NAD(P)H:quinone oxidoreductase 1) by both immunoblotting and immunohistochemistry staining (Fig. 6A and B, bottom panels). Taken together, Sag transgenic expression altered multiple

signaling pathways mainly via promoting ubiquitylation and degradation of selective sets of substrates, leading to inactivation of the mTORC1 pathway, which likely contributes to reduced proliferation and pancreas atrophy in KCS mice.

Discussion

SAG/RBX2 is a dual E3 for neddylation and ubiquitylation: when coupled with UBE2F neddylation E2, SAG acts as a neddylation E3 to promote cullin-5 neddylation; when coupled with ubiquitylation E2s, UBE2C/UBE2S or UBCH5C, SAG formed complex with cullin-5 or cullin-1, respectively and acts as ubiquitylation E3 to promote ubiquitylation and degradation of many substrates [5,10,32]. Our previous study showed that SAG is overexpressed in various human cancers, and SAG silencing inhibits pancreatic cancer cell growth both *in vitro* and in an

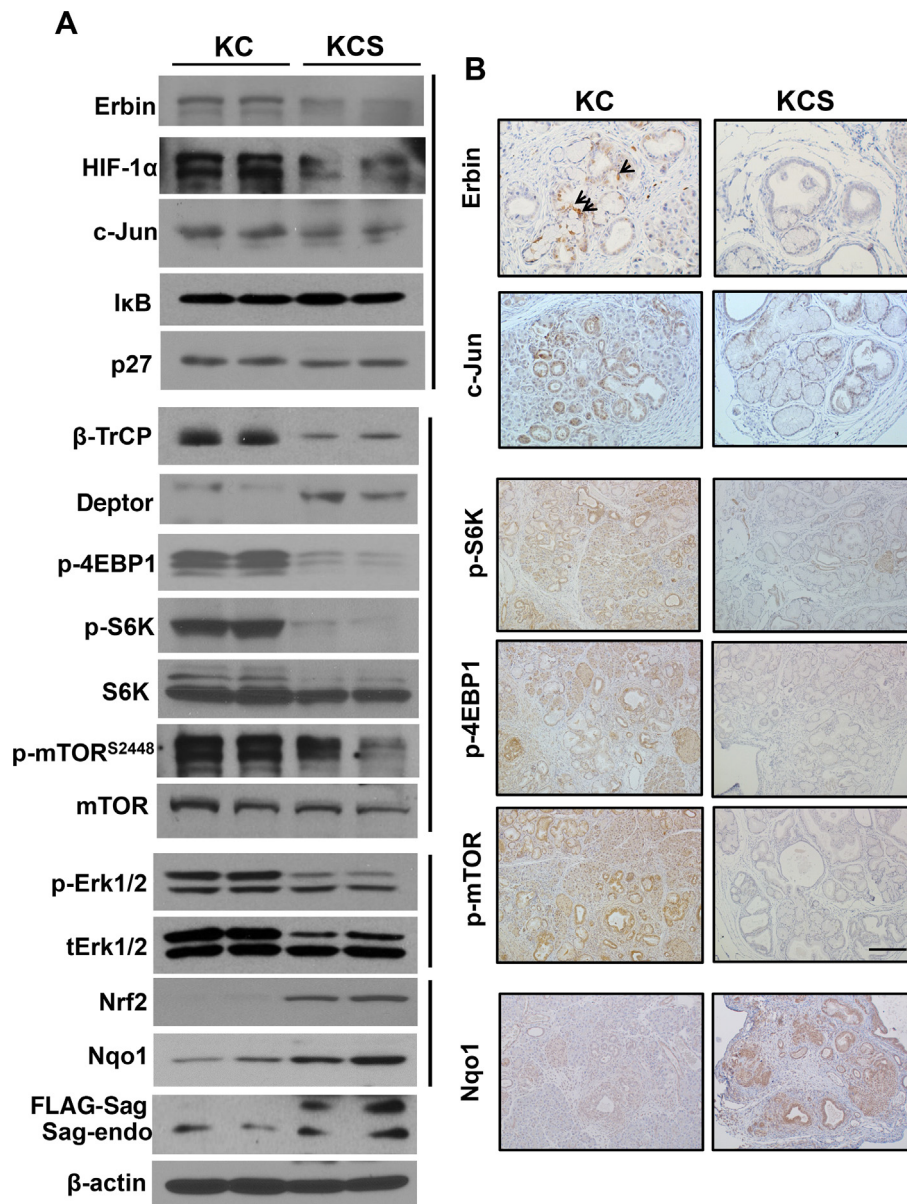


Fig. 6. SAG transgenic expression altered multiple signal pathways. (A) Western blot analysis of the indicated proteins in lysates of pancreatic tissues from two independent 6-month-old KC and KCS mice. (B) Immunohistochemical assessment of c-Jun, Erbin, p-S6K, p-4EBP1, and p-mTOR in KC and KCS pancreata at 6 months of age. Scale bar, 100 μ m.

orthotopic *in vivo* mouse model [5,13]. In line with these observations, here we show with cancer database profiling that SAG is overexpressed in a cohort of human PDAC samples, and higher SAG expression levels are associated with poor prognosis in PDAC patients. However, it is previously unknown whether this overexpressed SAG indeed plays a causal role in pancreatic tumorigenesis.

To this end, we generated two SAG transgenic mouse lines with pancreas-selective expression driven by a 5.2 kb p48 promoter fragment upon Cre-mediated recombination. While mice with Sag transgenic expression in the pancreas alone develop normally without any visible abnormal phenotypes, Sag transgenic expression under the background of *Kras*^{G12D} (KCS) demonstrated many abnormal phenotypes, including atrophic pancreata with impaired pancreatic functions, smaller body size, and much shorter life-span. While Sag-transgenic expression indeed promotes the development of low-grade mPanIN structure (PanIN1a and 1b) at the early stage, no further development to high-grade mPanINs or PDAC was found. Instead, KCS mice at 6 months had profound pancreatic atrophy with variously sized cystic structures. Consistent with these abnormal pancreas features, the *in vitro* 3D-culture assay showed that Sag-transgenic expression accelerated ADM conversion with much enlarged duct-like structures. These results suggested that Sag transgenic expression accelerates the process of *Kras*-induced precursor lesions at the early stage, but altered the cell fate from neoplastic progression to cystogenesis, leading to the massive loss of acinar cells, reduced proliferation, atrophic pancreas with impaired pancreatic function, and eventually early death. The dual roles of Sag overexpression in *Kras*-mutated mouse pancreata implies that Sag might target different sets of substrates in a cell-context (acinar cells vs. intraepithelial neoplastic cells) dependent and time dependent manner. This is reminiscent of the role of Sag in skin carcinogenesis induced by DMBA/TPA, where Sag-transgenic expression leads to a reduced skin hyperplasia by targeting *c-Jun/AP-1* at the early stage, but enhanced tumor growth via activating NF- κ B by targeting I κ B to inhibit apoptosis at the later stage [16].

In an attempt to elucidate the underlying mechanisms of Sag action, we used immunoblotting and immunohistochemistry staining methods to measure the protein levels of several Sag substrates known to regulate cell growth or be responsive to stress in pancreatic tissues from KCS vs. KC mice. We found that while Sag transgenic expression did not affect the levels of p27 or I κ B, it did reduce the levels of Erbin, HIF-1 α , *c-Jun* and β -TrCP1. Furthermore, Sag transgenic expression increased the levels of Nrf2 and its transcriptional target, Nqo1. While reduced Erbin, an inhibitor of Ras activation of Raf [33], failed to cause activation of MAPK/pERK, the detailed biological significance of decreased HIF-1 α and *c-Jun* to KCS phenotype is unclear at the present time. Reduced *c-Jun* would inactivate AP-1 transcription factor, which could contribute to reduced proliferation.

Of particular interest is the finding that Sag-induced β -TrCP1 reduction, as a result of enhanced degradation [10], caused accumulation of Deptor, a well-known substrate of β -TrCP1 [27–29], resulting in inactivation of mTORC1 signaling. The mTORC1 pathway is well known for its ability to drive cell cycle progression and cell growth [34–36]. This observation might imply that the disease progression from the early stage to late stage of mPanIN, and from late stage of mPanIN to PDAC in KCS mice is blocked through inactivation of mTORC1/S6K/4EBP1 activity, which also may explain why the pancreata of KCS mice are atrophic with a significant reduction in Ki67 staining. It is noteworthy that whether biochemical mTORC1 inactivation is associated with biological pancreatic cystogenesis in the pancreata of KCS is unclear. In a rat model of polycystic kidney disease (PKD), an mTOR kinase inhibitor did slow the disease progression [37], and mTORC1 was found to suppress polycystin-1 expression to drive renal cyst formation [38]. Whether mTORC1 plays a tissue (kidney vs. pancreas)-dependent role in regulation of cystogenesis warrants a future investigation.

In addition, we also observed increased protein levels of the antioxidant protein Nrf2 and its transcription target Nqo1 in KCS pancreata. The abnormal expression and activation of Nrf2 has been observed at different stages of pancreatic cancer and correlated with its initiation, progression, metastasis, and chemoresistance [39,40]. Interestingly, Nrf2 also plays dual roles in pancreatic carcinogenesis. At the early stage, Nrf2 exerts a tumor-suppressive role through binding to antioxidant response elements (AREs) and promoting its downstream target gene expression, which regulates the cellular antioxidant/detoxification response [41]. At the late stage, however, Cullin3-Keap1 mutation and silencing are frequently observed, which cause Nrf2 accumulation, leading to pancreatic cancer cell metastasis and chemoresistance [39,42]. Thus, it is also possible that elevated Nrf2 resulting from Sag transgenic expression contributes to blockage of disease progression from the early precursor lesions.

How Sag transgenic expression causes Nrf2 accumulation is unclear. Our previous study using a *Kras*^{G12D} skin cancer model showed that Sag deletion triggered Nrf2 accumulation; whereas in a prostate cancer model triggered by *Pten* loss, Sag deletion caused Deptor accumulation [18]. These opposite results in other organs from this KCS-PDAC study further demonstrate that Sag indeed plays a tissue/context-dependent role. By tissue-specific targeting of a subset of its substrates, Sag could play an oncogene- or tumor suppressor-cooperating role in regulation of tumorigenesis. Indeed, Sag is pro-oncogenic in the lung [15] and tumor-suppressive in the skin [19] during *Kras*^{G12D}-induced tumorigenesis, and in the prostate, Sag is pro-oncogenic during tumorigenesis induced by *Pten* loss [18]. In this pancreatic KCS model, Sag appears to be a *Kras*-cooperating gene at the early stage, but tumor suppressive by inactivating mTORC1 signaling at the later stage.

Finally, it is worth noting that two-fold increase of Sag levels via transgenic expression (at the level comparable to endogenous, Fig. 2E) did cause biochemical changes in the levels of several key proteins, likely due to increased ligase activity of Sag-associated CRL E3s, which contributes to observed phenotypic changes, as shown in this study. This observation is consistent with our previous reports that SAG is stress inducible protein [5,43], and induced SAG in response to stressed conditions, such as mitogen stimulation, hypoxia exposure or ROS, did cause enhanced degradation of several substrates, such as *c-JUN* and I κ B α [16,21,25,26]. On the other hand, Sag deletion caused accumulation of its substrates in a context dependent manner, again leading to phenotypic changes [15,18,19,44].

In summary, our study demonstrates that pancreatic specific Sag transgenic expression in combination with *Kras*^{G12D} promotes ADM and early mPanIN formation, but without preceding to later stage mPanINs, nor adenocarcinoma. Instead, Sag transgenic expression at the later stage caused acinar cell loss, pancreatic atrophy, and pancreatic cystogenesis, which could be attributable to alterations in multiple signaling pathways including the β -TrCP1/Deptor/mTOR axis and Nrf2 accumulation. The future study is directed toward delineating the detailed molecular mechanisms of Sag in different stages of pancreatic tumorigenesis and progression using rescuing approaches.

Acknowledgement

This work was supported by NCI grant 1R21CA170995 to YS.

Authors' contributions

Q.Z. and Y.S. conceived and designed the experiments. Q.Z. D.W., and M.T. performed the experiments. All the authors analyzed the data. M.M. and Y.S. supervised the study. Q.Z. and Y.S. wrote the paper. All authors reviewed and approved the manuscript before submission.

Competing interests

The authors declare that they have no competing interests.

References

1. Siegel RL, Miller KD, Jemal A. Cancer statistics, 2020. *CA Cancer J Clin* 2020;**70**(1):7–30.
2. Fitzgerald TL, Lertpiriyapong K, Cocco L, Martelli AM, Libra M, Candido S, Montalto G, Cervello M, Steelman L, Abrams SL, et al. Roles of EGFR and KRAS and their downstream signaling pathways in pancreatic cancer and pancreatic cancer stem cells. *Adv Biol Regul* 2015;**59**:65–81.
3. Hezel AF, Kimmelman AC, Stanger BZ, Bardeesy N, Depinho RA. Genetics and biology of pancreatic ductal adenocarcinoma. *Genes Dev* 2006;**20**(10):1218–49.
4. Hingorani SR, Petricoin EF, Maitra A, Rajapakse V, King C, Jacobetz MA, Ross S, Conrads TP, Veenstra TD, Hitt BA, et al. Preinvasive and invasive ductal pancreatic cancer and its early detection in the mouse. *Cancer Cell* 2003;**4**(6):437–50.
5. Sun Y, Li H. Functional characterization of SAG/RBX2/ROC2/RNF7, an antioxidant protein and an E3 ubiquitin ligase. *Protein Cell* 2013;**4**(2):103–16.
6. Sun Y, Tan M, Duan H, Swaroop M. SAG/ROC/Rbx/Hrt, a zinc RING finger gene family: molecular cloning, biochemical properties, and biological functions. *Antioxid Redox Signal* 2001;**3**(4):635–50.
7. Jin J, Cardozo T, Lovering RC, Elledge SJ, Pagano M, Harper JW. Systematic analysis and nomenclature of mammalian F-box proteins. *Genes Dev* 2004;**18**(21):2573–80.
8. Tan M, Davis SW, Saunders TL, Zhu Y, Sun Y. RBX1/ROC1 disruption results in early embryonic lethality due to proliferation failure, partially rescued by simultaneous loss of p27. *Proc Natl Acad Sci U S A* 2009;**106**(15):6203–8.
9. Tan M, Li Y, Yang R, Xi N, Sun Y. Inactivation of SAG E3 ubiquitin ligase blocks embryonic stem cell differentiation and sensitizes leukemia cells to retinoid acid. *PLoS One* 2011;**6**(11) e27726.
10. Kuang P, Tan M, Zhou W, Zhang Q, Sun Y. SAG/RBX2 E3 ligase complexes with UBCH10 and UBE2S E2s to ubiquitylate beta-TrCP1 via K11-linkage for degradation. *Sci Rep* 2016;**6**:37441.
11. Huang Y, Duan H, Sun Y. Elevated expression of SAG/ROC2/Rbx2/Hrt2 in human colon carcinomas: SAG does not induce neoplastic transformation, but its antisense transfection inhibits tumor cell growth. *Mol Carcinog* 2001;**30**:62–70.
12. Sasaki H, Yukiue H, Kobayashi Y, Moriyama S, Nakashima Y, Kaji M, Fukai I, Kiriyama M, Yamakawa Y, Fujii Y. Expression of the sensitive to apoptosis gene, SAG, as a prognostic marker in nonsmall cell lung cancer. *Int J Cancer* 2001;**95**(6):375–7.
13. Jia L, Yang J, Hao X, Zheng M, He H, Xiong X, Xu L, Sun Y. Validation of SAG/RBX2/ROC2 E3 Ubiquitin ligase as an anticancer and radiosensitizing target. *Clin Cancer Res* 2010;**16**(3):814–24.
14. Mega Tiber P, Baloglu L, Ozden S, Ozgen Z, Ozyurt H, Eren M, Orun O. The association of apoptotic protein expressions sensitive to apoptosis gene, p73 and p53 with the prognosis of cervical carcinoma. *Oncotargets Ther* 2014;**7**:2161–8.
15. Li H, Tan M, Jia L, Wei D, Zhao Y, Chen G, Xu J, Zhao L, Thomas D, Beer DG, et al. Inactivation of SAG/RBX2 E3 ubiquitin ligase suppresses KrasG12D-driven lung tumorigenesis. *J Clin Invest* 2014;**124**(2):835–46.
16. Gu Q, Bowden GT, Normolle D, Sun Y. SAG/ROC2 E3 ligase regulates skin carcinogenesis by stage-dependent targeting of c-Jun/AP1 and IkappaB-alpha/NF-kappaB. *J Cell Biol* 2007;**178**(6):1009–23.
17. He H, Gu Q, Zheng M, Normolle D, Sun Y. SAG/ROC2/RBX2 E3 ligase promotes UVB-induced skin hyperplasia, but not skin tumors, by simultaneously targeting c-Jun/AP-1 and p27. *Carcinogenesis* 2008;**29**(4):858–65.
18. Tan M, Xu J, Siddiqui J, Feng F, Sun Y. Depletion of SAG/RBX2 E3 ubiquitin ligase suppresses prostate tumorigenesis via inactivation of the PI3K/AKT/mTOR axis. *Mol Cancer* 2016;**15**(1):81.
19. Xie CM, Wei D, Zhao L, Marchetto S, Mei L, Borg JP, Sun Y. Erbin is a novel substrate of the Sag-betaTrCP E3 ligase that regulates KrasG12D-induced skin tumorigenesis. *J Cell Biol* 2015;**209**(5):721–38.
20. Zhang Q, Zhang Y, Parsels JD, Lohse I, Lawrence TS, Pasca di Magliano M, Sun Y, Morgan MA. Fbxw7 Deletion accelerates Kras(G12D)-driven pancreatic tumorigenesis via yap accumulation. *Neoplasia* 2016;**18**(11):666–73.
21. Gu Q, Tan M, Sun Y. SAG/ROC2/Rbx2 is a novel activator protein-1 target that promotes c-Jun degradation and inhibits 12-O-tetradecanoylphorbol-13-acetate-induced neoplastic transformation. *Cancer Res* 2007;**67**(8):3616–25.
22. Badea L, Herlea V, Dima SO, Dumitrascu T, Popescu I. Combined gene expression analysis of whole-tissue and microdissected pancreatic ductal adenocarcinoma identifies genes specifically overexpressed in tumor epithelia. *Hepatogastroenterology* 2008;**55**(88):2016–27.
23. Haerberle L, Esposito I. Pathology of pancreatic cancer. *Transl Gastroenterol Hepatol* 2019;**4**:50.
24. Rachagani S, Torres MP, Kumar S, Haridas D, Baine M, Macha MA, Kaur S, Ponnusamy MP, Dey P, Seshacharyulu P, et al. Mucin (Muc) expression during pancreatic cancer progression in spontaneous mouse model: potential implications for diagnosis and therapy. *J Hematol Oncol* 2012;**5**:68.
25. Tan M, Zhu Y, Kovacev J, Zhao Y, Pan ZQ, Spitz DR, Sun Y. Disruption of Sag/Rbx2/Roc2 induces radiosensitization by increasing ROS levels and blocking NF-kB activation in mouse embryonic stem cells. *Free Radical Biol Med* 2010;**49**(6):976–83.
26. Tan M, Gu Q, He H, Pamarthy D, Semenza GL, Sun Y. SAG/ROC2/RBX2 is a HIF-1 target gene that promotes HIF-1alpha ubiquitination and degradation. *Oncogene* 2008;**27**(10):1404–11.
27. Duan S, Skaar JR, Kuchay S, Toschi A, Kanarek N, Ben-Neriah Y, Pagano M. mTOR generates an auto-amplification loop by triggering the betaTrCP- and CK1alpha-dependent degradation of DEPTOR. *Mol Cell* 2011;**44**(2):317–24.
28. Gao D, Inuzuka H, Tan MK, Fukushima H, Locasale JW, Liu P, Wan L, Zhai YR, Chin YR, Shaik S, et al. mTOR drives its own activation via SCF (betaTrCP)-dependent degradation of the mTOR inhibitor DEPTOR. *Mol Cell* 2011;**44**(2):290–303.
29. Zhao Y, Xiong X, Sun Y. DEPTOR, an mTOR inhibitor, is a physiological substrate of SCFbetaTrCP E3 ubiquitin ligase and regulates survival and autophagy. *Mol Cell* 2011;**44**(2):304–16.
30. Peterson TR, Laplante M, Thoreen CC, Sancak Y, Kang SA, Kuehl WM, Gray DM, Sabatini DM. DEPTOR is an mTOR inhibitor frequently overexpressed in multiple myeloma cells and required for their survival. *Cell* 2009;**137**(5):873–86.
31. Sporn MB, Liby KT. NRF2 and cancer: the good, the bad and the importance of context. *Nat Rev Cancer* 2012;**12**(8):564–71.
32. Zhang S, Sun Y. Cullin RING Ligase 5 (CRL-5): neddylation activation and biological functions. *Adv Exp Med Biol* 2020;**1217**:261–83.
33. Dai P, Xiong WC, Mei L. Erbin inhibits RAF activation by disrupting the sur-8-Ras-Raf complex. *J Biol Chem* 2006;**281**(2):927–33.
34. Efeyan A, Sabatini DM. mTOR and cancer: many loops in one pathway. *Curr Opin Cell Biol* 2010;**22**(2):169–76.
35. Zoncu R, Efeyan A, Sabatini DM. mTOR: from growth signal integration to cancer, diabetes and ageing. *Nat Rev Mol Cell Biol* 2011;**12**(1):21–35.
36. Kim J, Guan KL. mTOR as a central hub of nutrient signalling and cell growth. *Nat Cell Biol* 2019;**21**(1):63–71.
37. Ravichandran K, Zafar I, Ozkok A, Edelstein CL. An mTOR kinase inhibitor slows disease progression in a rat model of polycystic kidney disease. *Nephrol Dial Transplant* 2015;**30**(1):45–53.
38. Pema M, Drusian L, Chiaravalli M, Castelli M, Yao Q, Ricciardi S, Somlo S, Qian F, Biffo S, Boletta A. mTORC1-mediated inhibition of polycystin-1 expression drives renal cyst formation in tuberous sclerosis complex. *Nat Commun* 2016;**7**:10786.
39. Chio IIC, Jafarnejad SM, Ponz-Sarvisse M, Park Y, Rivera K, Palm W, Wilson V, Sangar V, Hao Y, Ohlund D, et al. NRF2 promotes tumor maintenance by modulating mRNA translation in pancreatic cancer. *Cell* 2016;**166**(4):963–76.
40. Lister A, Nedjadi T, Kitteringham NR, Campbell F, Costello E, Lloyd B, Cople IM, Williams S, Owen A, Neoptolemos JP, et al. Nrf2 is overexpressed in pancreatic cancer: implications for cell proliferation and therapy. *Mol Cancer* 2011;**10**:37.
41. Thimmulappa RK, Mai KH, Srisuma S, Kensler TW, Yamamoto M, Biswal S. Identification of Nrf2-regulated genes induced by the chemopreventive agent sulforaphane by oligonucleotide microarray. *Cancer Res* 2002;**62**(18):5196–203.

42. Qin JJ, Cheng XD, Zhang J, Zhang WD. Dual roles and therapeutic potential of Keap1-Nrf2 pathway in pancreatic cancer: a systematic review. *Cell Commun Signal* 2019;**17**(1):121.
43. Duan H, Wang Y, Aviram M, Swaroop M, Loo JA, Bian J, Tian Y, Mueller T, Bisgaier CL, Sun Y. SAG, a novel zinc RING finger protein that protects cells from apoptosis induced by redox agents. *Mol Cell Biol* 1999;**19**:3145–55.
44. Tan M, Zhao Y, Kim SJ, Liu M, Jia L, Saunders TL, Zhu Y, Sun Y. SAG/RBX2/ROC2 E3 ubiquitin ligase is essential for vascular and neural development by targeting NF1 for degradation. *Dev Cell* 2011;**21**(6):1062–76.